

**NANO EXPRESS**

**Open Access**

# Inorganic nanotubes reinforced polyvinylidene fluoride composites as low-cost electromagnetic interference shielding materials

Varrla Eswaraiah<sup>1,2</sup>, Venkataraman Sankaranarayanan<sup>2</sup>, Sundara Ramaprabhu<sup>1\*</sup>

## Abstract

Novel polymer nanocomposites comprising of MnO<sub>2</sub> nanotubes (MNTs), functionalized multiwalled carbon nanotubes (*f*-MWCNTs), and polyvinylidene fluoride (PVDF) were synthesized. Homogeneous distribution of *f*-MWCNTs and MNTs in PVDF matrix were confirmed by field emission scanning electron microscopy. Electrical conductivity measurements were performed on these polymer composites using four probe technique. The addition of 2 wt.% of MNTs (2 wt.% *f*-MWCNTs) to PVDF matrix results in an increase in the electrical conductivity from 10<sup>-16</sup>S/m to 4.5 × 10<sup>-5</sup>S/m (3.2 × 10<sup>-1</sup>S/m). Electromagnetic interference shielding effectiveness (EMI SE) was measured with vector network analyzer using waveguide sample holder in X-band frequency range. EMI SE of approximately 20 dB has been obtained with the addition of 5 wt.% MNTs-1 wt.% *f*-MWCNTs to PVDF in comparison with EMI SE of approximately 18 dB for 7 wt.% of *f*-MWCNTs indicating the potential use of the present MNT/*f*-MWCNT/PVDF composite as low-cost EMI shielding materials in X-band region.

## Introduction

In recent years, electronics field has diversified in telecommunication systems, cellular phones, high-speed communication systems, military devices, wireless devices, etc. Due to the increase in use of high operating frequency and bandwidth in electronic systems, there are concerns and more chances of deterioration of the radio wave environment known as electromagnetic interference (EMI). This EMI has adverse effects on electronic equipments such as false operation due to unwanted electromagnetic waves and leakage of information in wireless telecommunications [1]. Hence, in order to maintain the electromagnetic compatibility of the end product, light weight EMI shielding materials are required to sustain the good working environment of the devices. EMI shielding refers to the reflection or absorption or multiple reflection of the electromagnetic radiation by a shielding material which thereby acts as a shield against the penetration of the radiation through it [2]. Conventionally, metals and metallic composites are

used as EMI shielding materials as they have high shielding efficiency owing to their good electrical conductivity. Even though metals are good for EMI shielding, they suffer from poor chemical resistance, oxidation, corrosion, high density, and difficulty in processing [3]. The chemical resistance of polymer is defined largely by its chemical structure. In the present case, polyvinylidene fluoride (PVDF) has been chosen as the base polymer because of its excellent chemical resistance [4,5] over a variety of chemicals, acids, and bases. It is well known that the addition of lower amount of inorganic nanotubes (1-10 wt.%) will not affect the basic properties such as chemical resistance, strength, etc. of the base polymer [6,7]. Ever since the discovery by Ijima [8], carbon nanotubes (CNT) have attracted considerable research interest owing to their unique physical and chemical properties [9,10]. CNT-polymer composites gained popularity recently for various applications [11-13] due to the distinct advantages of polymers and nanofillers (CNT) such as lightweight, resistance to corrosion, and chemical resistance of the polymer as well as high electrical conductivity, high aspect ratio, and high mechanical strength of CNT [14,15].

Previous studies on CNT-polymer composites show that carbon nanotubes can be considered as advanced

\* Correspondence: ramp@iitm.ac.in

<sup>1</sup>Alternative Energy and Nanotechnology Laboratory (AENL), Nano Functional Materials, Technology Centre (NFMTC), Department of Physics, Indian Institute of Technology Madras, Chennai 600036, India  
Full list of author information is available at the end of the article

reinforcing materials possessing excellent electrical and mechanical properties and their unique one-dimensional structure [16,17] make them ideal for creating overlapping conductive network for high-performance EMI shielding at low loadings [18-21]. CNT-polymer composites either based on solvent casting or melt-based techniques have been studied with various polymer matrices, including PMMA [22], liquid crystal polymers, and melamine formaldehydes [23], PVA [24], and fused silica [25] for various applications such as radiation protection, EMI shielding, and electrostatic discharge materials. There are many reports on EMI shielding of carbon nanotubes reinforced polymer composites [26-30] in the X-band region because of its use in military communication satellites, weather monitoring, air traffic control, defense tracking and high-resolution imaging radars. But the disadvantage is the high loading of carbon nanotubes which is at present economically not feasible. So, there is a critical need for the development of low-cost EMI shielding materials at this particular frequency. Yonglai et al. [31] reported low-cost EMI shielding materials with the combination of carbon nanofiber and carbon nanotube composites in polystyrene (PS) matrix. They could achieve electromagnetic interference shielding effectiveness (EMI SE) of 20 dB for the combination of 10 wt.% carbon nanofiber and 1 wt.% carbon nanotubes in PS matrix in the range 12-18 GHz. In the present study, we have developed a low-cost hybrid EMI shielding material comprising of manganese dioxide nanotubes and low loading of multiwalled carbon nanotubes (MWCNTs) in PVDF matrix. EMI shielding efficiency and electrical conductivity of the composites with different weight fractions of functionalized multiwalled carbon nanotubes (*f*-MWCNTs) and MnO<sub>2</sub> nanotubes (MNTs) were investigated to optimize polymer composites with less content of carbon nanotubes that exhibit enhanced electrical properties and serve as a better EMI shielding material. The focus of the present work is to fill the space between the MNTs using a low weight percent of *f*-MWCNTs within the polymer matrix and thereby making utmost use of the advantages of *f*-MWCNTs and eventually achieve low-cost and improved EMI shielding materials.

## Experimental section

### Materials

PVDF was used as polymer matrix with a molecular weight of 100,000 g/mol and it was purchased from Alfa Aesar. MWCNTs were synthesized by chemical vapor deposition technique. MNTs were prepared by hydrothermal route and *N,N*-dimethyl formamide was used as the solvent for carbon nanotubes and MnO<sub>2</sub> nanotubes. Laboratory grade acids, bases, and organic solvents were used.

### Synthesis of functionalized multiwalled carbon nanotubes

MWCNTs were synthesized by chemical vapor deposition technique using misch metal (approximately 50% cerium and 25% lanthanum, with small amounts of neodymium and praseodymium)-based AB<sub>3</sub> alloy hydride catalysts [32]. The as-grown MWCNTs not only contain pure MWCNTs but also amorphous carbon, fullerenes, and other metal catalysts. In order to remove these catalytic impurities and amorphous carbon, air oxidation was performed at 350°C for 4 h followed by acid treatment in concentrated HNO<sub>3</sub>. After purification, MWCNTs were functionalized with 3:1 ratio of H<sub>2</sub>SO<sub>4</sub> and HNO<sub>3</sub> at 60°C for 6 h in order to impart hydroxyl and carboxyl functional groups over the side walls.

### Synthesis of MnO<sub>2</sub> nanotubes

MNTs were prepared by hydrothermal route [33]. Briefly, 0.608 g of KMnO<sub>4</sub> and 1.27 ml of HCl (37 wt.%) were added to 70 ml of de-ionized water with continuous stirring to form the precursor solution. After stirring, the solution was transferred to a teflon lined stainless steel autoclave with a capacity of 100 ml. The autoclave was kept in an oven at 140°C for 12 h and then cooled down to room temperature. The resulting brown precipitate was collected, rinsed, and filtered to a pH 7. The as-prepared powders were then dried at 80°C in air.

### Synthesis of *f*-MWCNTs-MNTs-PVDF composites

MNTs and *f*-MWCNTs reinforced polymer matrix composites were prepared by mixing the respective composite solutions at high-speed rotations per minute followed by solvent casting. Here, we describe the method of preparation of the composites. Initially, 10 mg of MNTs and 990 mg of polymer were dispersed separately in dimethylformamide (DMF) with the help of an ultrasonicator for 1 h at room temperature for the preparation of 1 wt.% MNTs in polymer matrix. These two solutions were mixed by sonicating together for 1 h and the composite solution was transferred to a melt mixer and stirred at room temperature at 4,000 rpm for 2 h and at 80°C for 30 min. The resulting solution was transferred into the beaker and kept in an oven to remove the solvent. Finally, dried thin films were put in a mold and pressed to form 1-mm thick structures. A similar procedure was followed for the preparation of functionalized multiwalled carbon nanotubes (*f*-MWCNTs)/PVDF composite films. For the preparation of *f*-MWCNTs/MNTs/PVDF composite, fixed amount of MNTs, *f*-MWCNTs, and PVDF were added to DMF separately for a desired composition, and the above-mentioned procedure was followed to prepare the composite films. A series of composites were prepared in a similar way by varying the amount of polymer, MNTs, and MWCNTs.

### Characterization

The direct current (DC) volume electrical conductivity of the composites was measured at room temperature using homemade resistivity setup with the help of Keithley 2400 sourcemeter and 2182 nanovoltmeter. The high resistance of the films was measured with a 617 programmable electrometer and a 6517B high-resistance electrometer. The EMI shielding measurement was performed with an Agilent E8362B vector network analyzer using a 201-point averaging in the frequency range of 8 to 12 GHz (X-band). Figure 1 shows the pictorial representation of the experimental setup for measuring the shielding effectiveness of the composite materials. Here, we followed the transmission line technique using an X-band waveguide sample holder for measuring scattering parameters of the composites. Samples of dimensions  $22.84 \times 10.16 \text{ mm}^2$  were prepared and kept inside the waveguide. The EMI shielding effectiveness is defined as the ratio of incoming ( $P_i$ ) to outgoing power ( $P_o$ ) of radiation. Shielding effectiveness (SE) =  $10 \log (P_i/P_o)$  and is defined in decibels (dB). The higher the value in decibels, the less energy passes through the material. When electromagnetic radiation falls on the shielding material, reflection, absorption, and transmission are observed. The corresponding reflectivity ( $R$ ), absorptivity ( $A$ ), and transmissivity ( $T$ ) are according to the equation  $A + R + T = 1$ .  $R$  and  $T$  can be calculated from the measured scattering coefficients, from the relations  $S_{12} = 10 \log T$  and  $S_{11} = 10 \log R$ . The cross-sectional morphology of the composites were observed using field emission scanning electron microscope (FESEM, QUANTA 3 D, FEI) and transmission electron

microscope. X-ray elemental mapping was also performed using EDX genesis software. Powder X-ray diffraction (XRD) studies were carried out using X'Pert PRO, PANalytical diffractometer with nickel filter  $\text{Cu K}\alpha$  radiation as the X-ray source. The samples were scanned in steps of  $0.016^\circ$  in the  $2\theta$  range 10 to 80. For the determination of functional groups, a Fourier transform infrared spectrum was acquired using Perkin Elmer FTIR spectrometer from 400 to  $4,000 \text{ cm}^{-1}$ . The chemical resistance of the composites in different acids, bases, alkanes and organic solvents was estimated by measuring the weight of the sample before and after treatment with these chemicals using METTLER TOLEDO XS 105 weighing balance.

### Results and discussion

#### X-ray diffraction analysis

The crystal structure of polymer, MNTs, and  $f$ -MWCNTs has been investigated by powder X-ray diffraction. Figure 2 shows the XRD pattern of the PVDF,  $f$ -MWCNTs, and MNTs. Figure 2a shows the XRD pattern of  $f$ -MWCNTs in which the peaks are indexed to the reflections of hexagonal graphite. The absence of additional peaks corresponding to the catalytic impurities confirms that the impurities have been removed by the acid treatment. The XRD spectrum of the as-synthesized MNT is shown in Figure 2b. All the diffraction peaks can be indexed according to the  $\alpha\text{-MnO}_2$  phase, and no other characteristic peaks from any impurity are observed. This establishes the high purity of the sample. In Figure 2c, it can be seen that pure PVDF membrane is crystalline in nature with visible peaks at  $18.65^\circ$  and

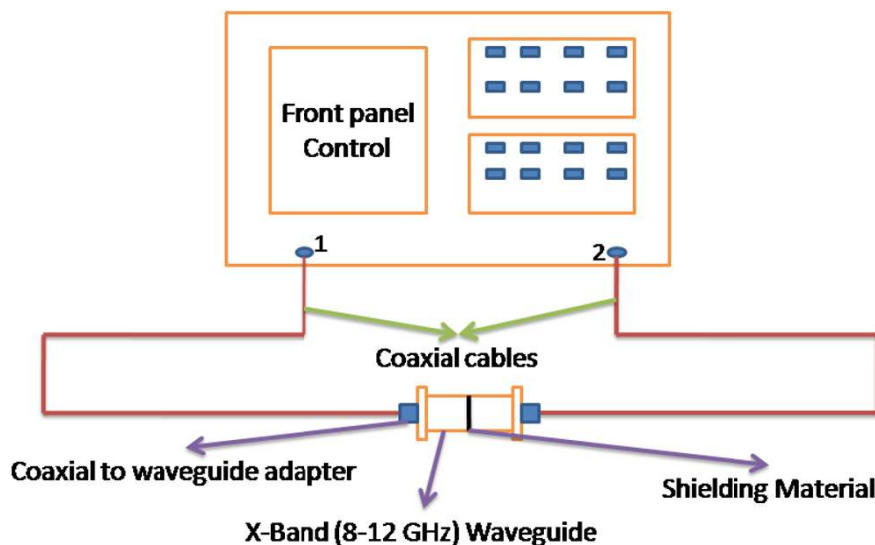
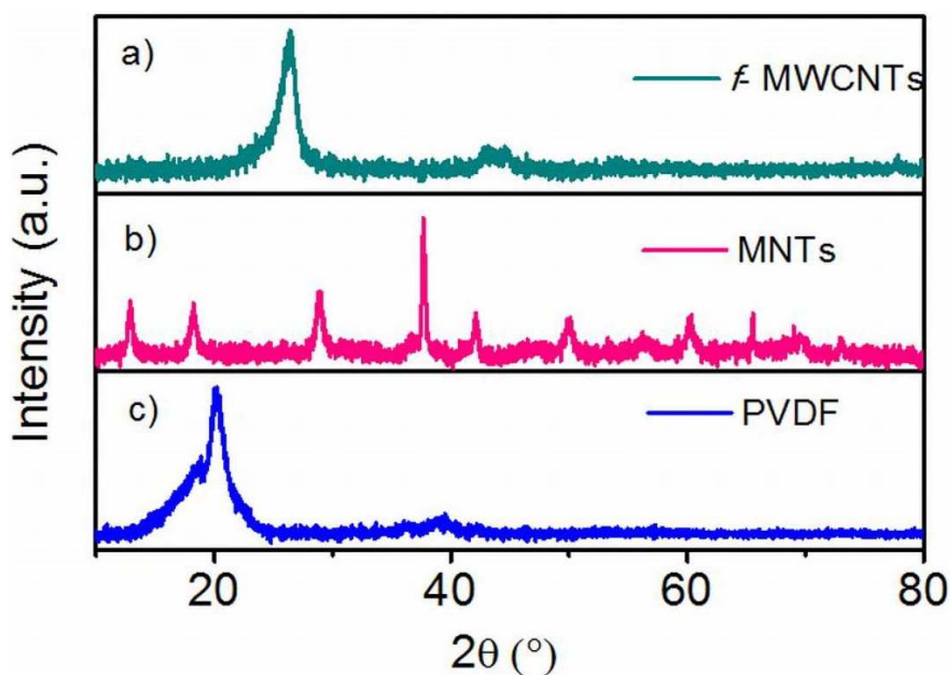


Figure 1 Experimental setup for EMI shielding characteristic measurements of polymer composites.



**Figure 2** X-ray diffractograms of *f*-MWCNTs, MNTs, and PVDF.

20.09°. The sharp peak at 20.09° can be attributed to the presence of  $\beta$ -polymorph.

#### Fourier transform infrared analysis

Figure 3 shows the FTIR spectra of purified and functionalized MWCNTs (*f*-MWCNTs). The broad absorption band at  $3,438\text{ cm}^{-1}$  is attributed to the hydroxyl group ( $\nu\text{OH}$ ). The asymmetric and symmetric stretching of CH bonds are observed at  $2,927$  and  $2,853\text{ cm}^{-1}$ , respectively and the stretching of C = O of the carboxylic acid (-COOH) group is observed at  $1,734\text{ cm}^{-1}$ . The stretching of C = C, O-H bending deformation in -COOH and CO bond stretching in the *f*-MWCNTs are observed at  $1,635\text{ cm}^{-1}$ ;  $1,436\text{ cm}^{-1}$ ; and  $1,073\text{ cm}^{-1}$ ; respectively indicating that carboxyl and hydroxyl functional groups were attached to the surface of MWCNTs.

#### Raman spectra analysis

Figure 4 shows the Raman spectra of purified and functionalized MWCNTs. The spectra consists of three main peaks. The peak at  $1,343\text{ cm}^{-1}$  is assigned to the defects and disordered graphite structures, while the peaks at  $1,586\text{ cm}^{-1}$  and  $2,693\text{ cm}^{-1}$  are attributed to the graphite band which is common to all  $\text{sp}^2$  systems and second-order Raman scattering process, respectively. Intensity ratio of defect band and graphite band is a signature of the degree of functionalization of the MWCNTs. As seen from Figure 4,  $I_D/I_G$  of pure carbon nanotubes is

0.868 whereas that for functionalized carbon nanotubes is 0.928 indicating the more defective nature of *f*-MWCNTs.

#### Morphology and composition analysis

Morphology is an important factor which affects the EMI SE of the composites. Figure 5a, b, c, d, e, f shows the FESEM images of polymer, nanofillers and nanofiller reinforced polymer composites. The corresponding images are (a) pure PVDF, (b) *f*-MWCNTs, (c) pure MNTs, (d) 1 wt.% MNTs-PVDF composite, (e) 2 wt.% MNTs-PVDF composite, and (f) high resolution image of 2 wt.% MNTs-PVDF composite. As shown in the Figure 5b and c, MWCNTs are 30 to 40 nm in diameter and approximately 10  $\mu\text{m}$  in length and MNTs are 50 to 70 nm in diameter and in micron length. It can be observed that MWCNTs are entangled with each other because of Van der Waals interactions, whereas manganese dioxide nanotubes were straight and rigid and PVDF shows smooth surface as shown in the Figure 5a. *f*-MWCNTs and MNTs were homogeneously distributed and embedded in the PVDF matrix as shown in Figure 6a, b, c, d, e, f due to ultrasonication and shear mixing of the solutions at high rpm in the formation of composite films. Figure 6d, e, f indicates that the space between filler aggregates in carbon nanotube-PVDF composites is much smaller than that of MNTs-PVDF composites. Figure 6e shows the FESEM image of 5 wt.



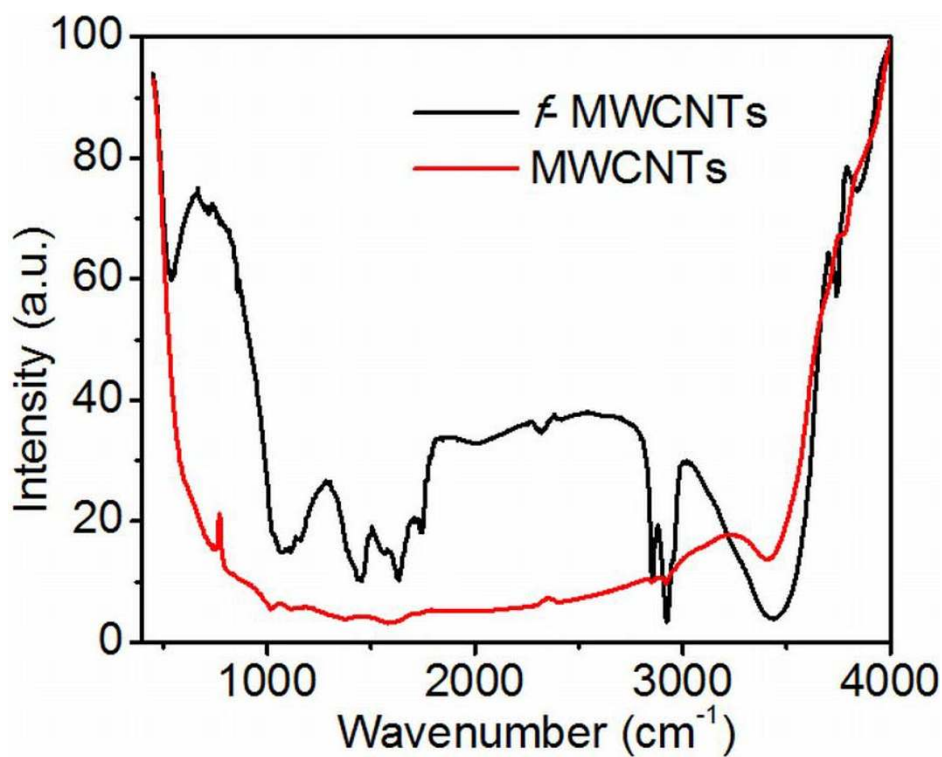


Figure 3 FTIR spectra of purified and functionalized MWCNTs.

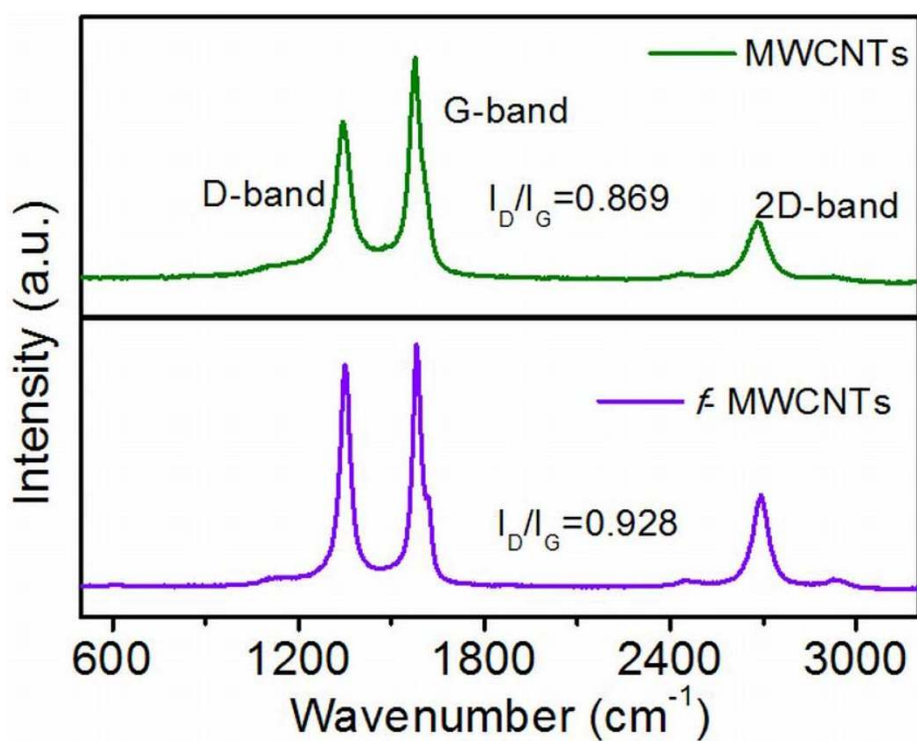
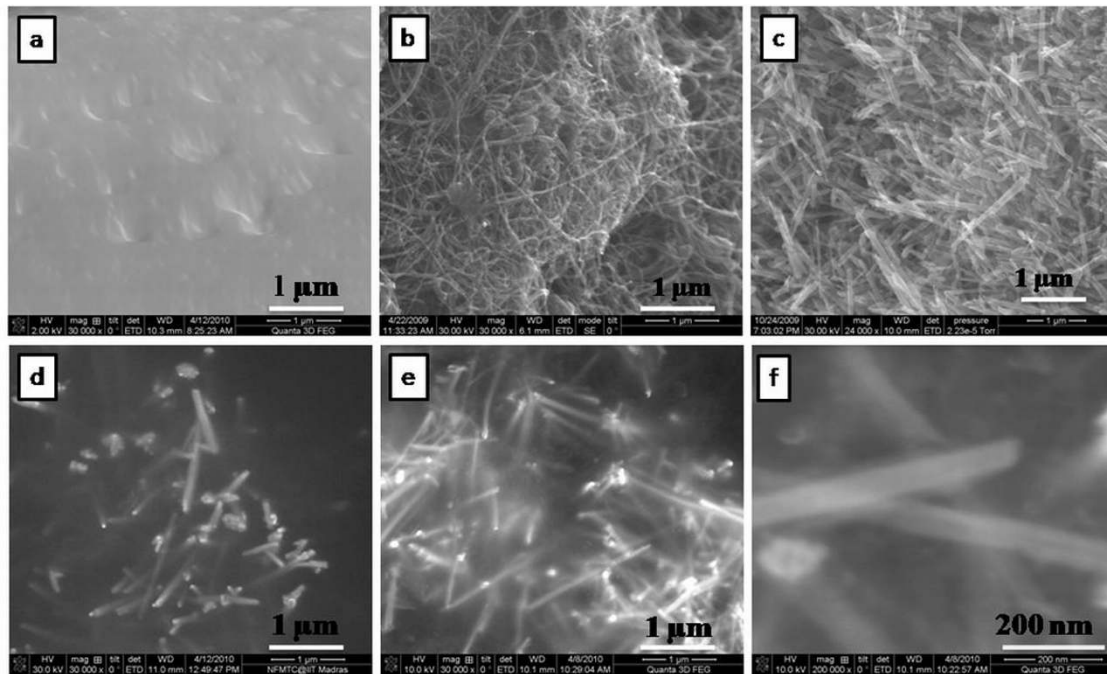


Figure 4 Raman spectra of purified and functionalized MWCNTs.



**Figure 5** Field emission scanning electron microscope images. (a) PVDF, (b) *f*-MWCNTs, (c) MNTs, (d) 1 wt.% MNTs-PVDF, (e) 2 wt.% MNTs-PVDF, and (f) high-resolution image of 2 wt.% *f*-MWCNTs-PVDF.

% MNTs filled PVDF composite along with 1 wt.% MWCNTs. It is observed that a very good microstructure has been formed, and *f*-MWCNTs were uniformly dispersed and embedded between the MNTs throughout the PVDF matrix. This good network can increase the

number of inter nanostructure connections, and hence provide better EMI SE. Further, to confirm the homogeneity of the composites, we have performed X-ray elemental mapping over the sample surface to visualize the atomic elements of manganese, oxygen, carbon, and

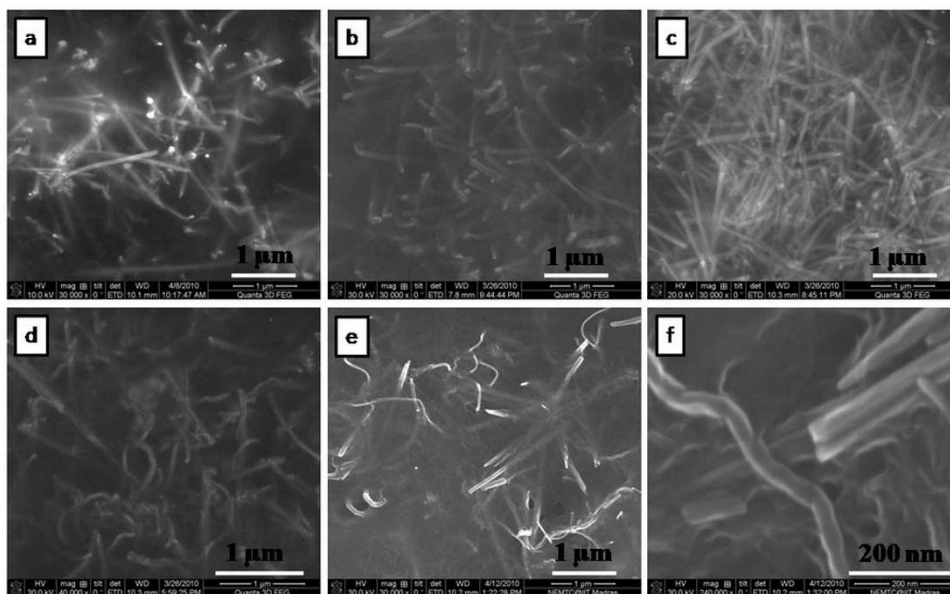


**Figure 6** Field emission scanning electron microscope images. (a) 3 wt.% MNTs-PVDF, (b) 4 wt.% MNTs-PVDF, (c) 5 wt.% MNTs-PVDF, (d) 1 wt.% *f*-MWCNTs-5 wt.% MNTs-PVDF, (e) 2 wt.% *f*-MWCNTs-5 wt.% MNTs-PVDF, and (f) high-resolution image of 1 wt.% *f*-MWCNTs-5 wt.% MNTs-PVDF.

fluorine. Figure 7 shows the EDX spectra of PVDF-based MNTs and *f*-MWCNTs composite. It confirms the presence of manganese and oxygen from MnO<sub>2</sub>, carbon from *f*-MWCNTs, and fluorine from the PVDF polymer. Figure 8 shows the elemental mapping of the 5 wt.% MNTs-1 wt.% *f*-MWCNTs-PVDF composite. As can be seen from the figures, all the elements were distributed homogeneously in the polymer matrix.

#### Chemical resistance of the polymer composites

The percentage of chemical resistance of the composites in different acids, bases, organic solvents, and alkanes are shown in the Table 1. It indicates that all the polymer composites are highly resistant towards the chemicals. The MNT-MWCNTs-PVDF composite shows 95% to 100% resistance towards chemicals which indicates the potentiality of the present composite. For comparison, the chemical resistances of MWCNT-PVDF, PVDF, and MNT-PVDF composites were also measured.

#### Electrical conductivity analysis

Electrical conductivity is of utmost importance for effective EMI shielding material. As shown in the Figure 9, the conductivity of the PVDF is about 10<sup>-16</sup>S/m. As the concentration of the MNTs increases in the PVDF matrix, electrical conductivity increases, and it follows percolation behavior. Conductivity of the 1 wt.% MNTs/PVDF composite was found to be approximately 10<sup>-6</sup>S/m, which indicates that there is a drastic improvement in electrical conductivity. An increase of about ten

orders of magnitude of electrical conductivity was observed which can be attributed to the high aspect ratio and efficient dispersion of the MNTs in the PVDF matrix. Similar trend is observed in the case of electrical conductivity of the *f*-MWCNTs/PVDF composites as shown in Figure 9b. The possible mechanism for the increment in the electrical conductivity of the composites can be the tunneling effect of the electrons from one nanotube to the other. The effect of *f*-MWCNTs content on the electrical conductivity of the MNTs/PVDF composites was studied. Incorporation of 1 wt.% *f*-MWCNTs in 5 wt.% MNT/PVDF composites increases the conductivity from 10<sup>-5</sup>S/m to approximately 10<sup>-1</sup>S/m which can be attributed to the high aspect ratio, homogeneous dispersion, and high electrical conducting nature of the *f*-MWCNTs.

#### Electromagnetic interference shielding effectiveness

The EMI SE of MNTs/PVDF composites with various mass fractions of MNTs as a function of frequency are presented in Figure 10a. The results show that EMI shielding effectiveness of pure PVDF is almost 0.3 dB indicating that it is transparent to the electromagnetic radiation throughout the measured frequency. This is probably due to its electrically insulating nature. It is observed that EMI SE starts increasing with the addition of MNTs to the insulating PVDF matrix. The EMI SE for 1 wt.% MNTs filled PVDF composite is found to be 2.27 dB and it increases further to 5.14 and 11 dB at higher loading of MNTs of 3 and 5 wt.%, respectively.

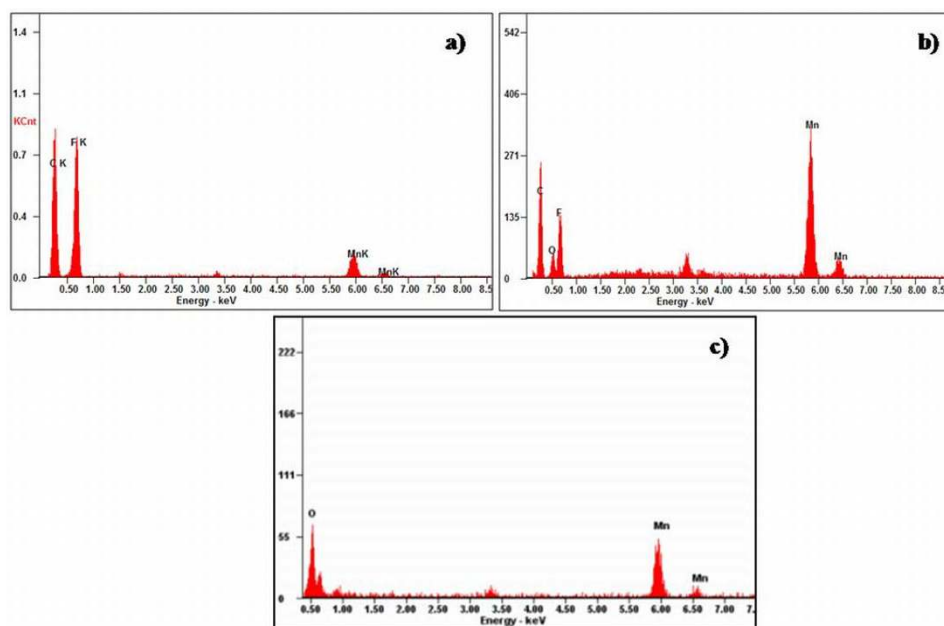
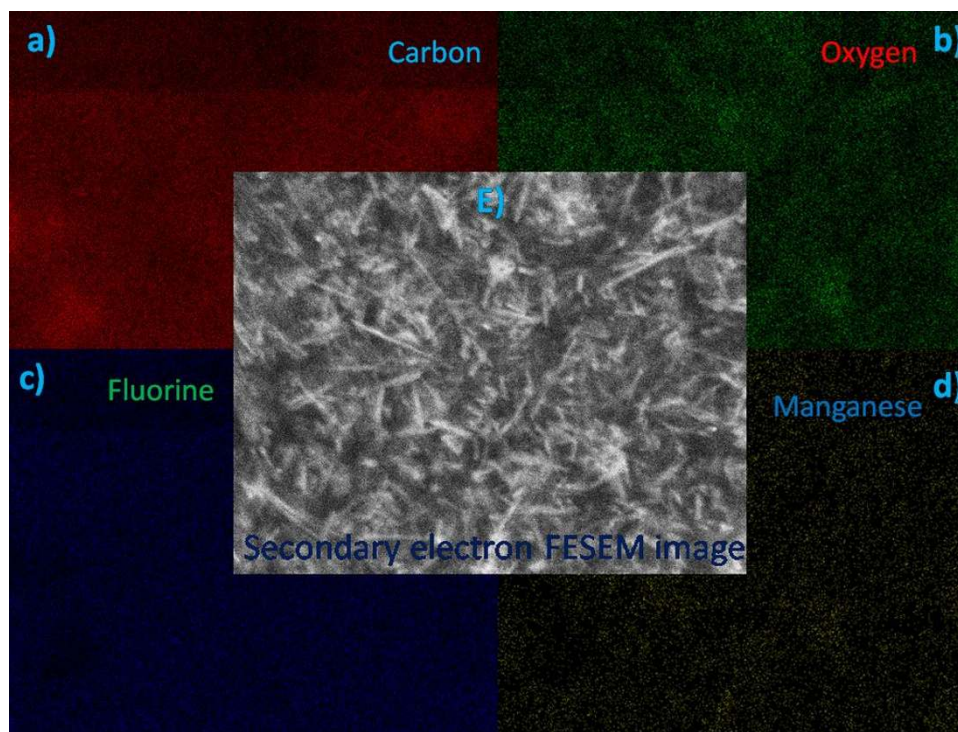


Figure 7 Energy dispersive X-ray spectra of MnO<sub>2</sub> nanotubes and its composites.





**Figure 8** X-ray elemental mapping of 5 wt.% MNT-1 wt.% *f*-MWCNTs-PVDF composite.

Hence, it is clear that the major contribution to the EMI shielding comes from the addition of semiconducting MNTs to the PVDF matrix. This increment in EMI SE can be attributed to the formation of conductive and connective network in the PVDF matrix, which is in accordance with the high-resolution FESEM image of MNTs filled PVDF composite (Figure 5f). Since electrical conductivity of the MNTs is two orders less

compared to that of carbon nanotubes, there is a limit over the highest obtainable conductivity of the total composite. This limits the EMI SE to approximately 12 dB for 5 wt.% MNTs/PVDF composite. These results suggest that the MNTs/PVDF composites can be used for electrostatic discharge applications. In order to make it suitable for EMI shielding applications, a small amount of (1 wt.%) *f*-MWCNTs have been incorporated in MNT/PVDF matrix. With this, 1 wt.% *f*-MWCNTs in 5 wt.% MNTs/PVDF composite, we could achieve an EMI SE of 18 to 22 dB. For comparison, the EMI SE of 7 wt.% *f*-MWCNTs/PVDF composites alone in the same frequency region has been measured, and in this case, an EMI SE of 18 dB has been obtained as shown in Figure 10c. Table 2 shows the overall EMI SE of different composites and their electrical conductivities. It is clear that 5 wt.% MNTs-1 wt.% *f*-MWCNTs-PVDF composite can be a better and low-cost EMI shielding material.

**Table 1** Percentage of chemical resistance for different polymer composites

Chemical	Percentage of chemical resistance			
	PVDF	5 wt.% MNT- <i>f</i> -MWCNT-PVDF	1 wt.% <i>f</i> -MWCNT-PVDF	5 wt.% MNT-PVDF
Acetic acid glacial	98.9	97.9	98.2	98.0
Oleic acid	100	100	98.5	100
Sodium hydroxide solution	97.6	96.0	98.8	97.2
Ammonia solution	98.7	98.4	95.7	96.8
n-Hexane	97.8	100.0	98.7	100
2-Propanol	98.9	100.0	98.3	97.3
Toluene	97.0	98.1	97.0	97.2
Chloroform	100	97.9	100	96.8

**Shielding mechanism in MNTs/*f*-MWCNTs/PVDF composites**

It is well reported that reflection is the most prominent EMI shielding mechanism in CNT-polymer composites [34]. In the present case, EMI shielding in *f*-MWCNTs reinforced PVDF composites has been studied and from the measured scattering parameters reflectivity, transmissivity, and absorptivity were derived using the



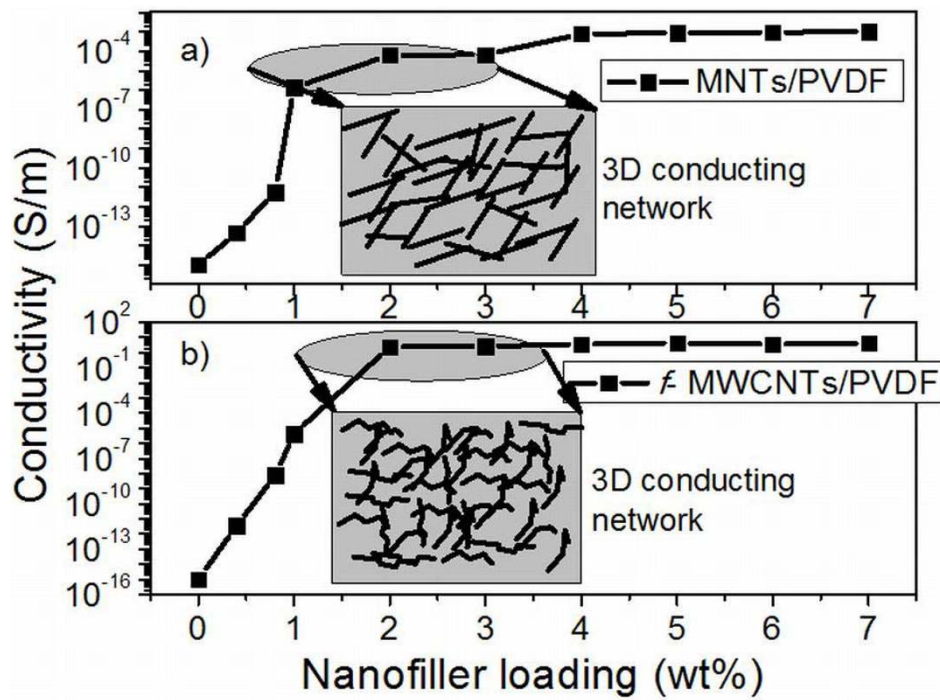


**Figure 9** DC electrical conductivity of the MNTs/PVDF and *f*-MWCNTs/PVDF composites.

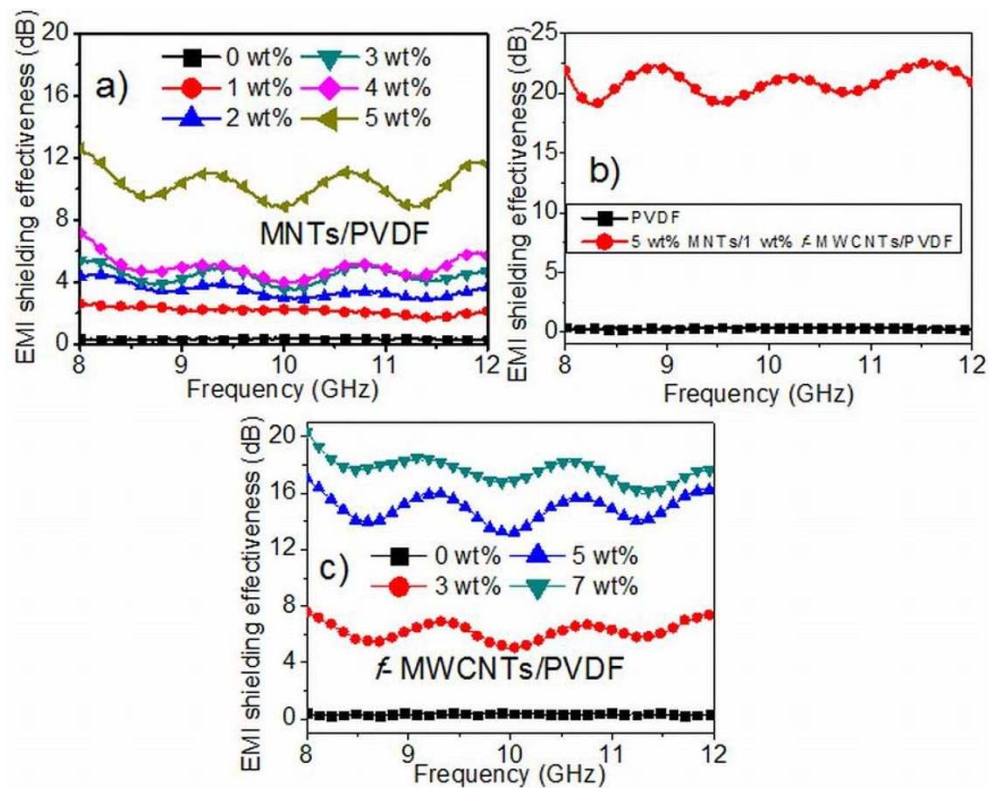


**Figure 10** EMI shielding effectiveness of MNTs/PVDF, MNTs/*f*-MWCNTs/PVDF and *f*-MWCNTs/PVDF composites.

**Table 2 Electrical conductivity and EMI SE of the polymer composites**

Composite	Electrical conductivity (S/m)	EMI SE (dB)
1 wt.% <i>f</i> -MWCNTs/PVDF	Approximately $10^{-10}$	Approximately 2
2 wt.% <i>f</i> -MWCNTs/PVDF	Approximately $10^{-1}$	Approximately 7
5 wt.% MNTs/PVDF	Approximately $10^{-5}$	Approximately 11
7 wt.% <i>f</i> -MWCNTs/PVDF	Approximately $10^{-1}$	Approximately 18
5 wt.% MNTs/1 wt.% <i>f</i> -MWCNTs/PVDF	Approximately $10^{-1}$	Approximately 21
5 wt.% MNTs/2 wt.% <i>f</i> -MWCNTs/PVDF	Approximately $10^{-1}$	Approximately 20

formulae mentioned in the experimental section. For 5 wt.% *f*-MWCNT-PVDF composites, the transmissivity, reflectivity, and absorptivity are 0.177, 0.601, and 0.222, respectively and the corresponding parameters for 7 wt.% *f*-MWCNT-PVDF composites are 0.131, 0.794, and 0.075. From these results, we can conclude that reflection is the major EMI shielding mechanism in the present *f*-MWCNT-PVDF composites. This may be due to the presence of conjugated  $\pi$  electrons on the surface of *f*-MWCNTs. In the case of MNTs/PVDF composites, the chances of absorbing incident radiation are more due to the presence of electric dipoles. Table 3 gives a comparison of the reflectivity and absorptivity of various composites. It is observed that *f*-MWCNTs/MNTs/PVDF composites and MNTs/PVDF composites exhibit more absorption than reflection. For 5 wt.% MNTs/1 wt.% *f*-MWCNTs/PVDF composite, the absorptivity, transmissivity, and reflectivity values are respectively 0.78, 0.01, and 0.210. Based on the measured fundamental properties of MNTs/PVDF, *f*-MWCNTs/PVDF, and MNTs/*f*-MWCNTs/PVDF composites, the present composites can be engineered for reflection to absorption of the incoming EM radiation by varying the amount of carbon nanotubes and MnO<sub>2</sub> nanotubes in the polymer

**Table 3 Transmissivity, reflectivity, and absorptivity of MNTs/*f*-MWCNTs/PVDF composites**

Composite	Absorptivity	Transmissivity	Reflectivity
1 wt.% <i>f</i> -MWCNTs/PVDF	0.042	0.631	0.327
2 wt.% <i>f</i> -MWCNTs/PVDF	0.218	0.199	0.583
5 wt.% <i>f</i> -MWCNTs-PVDF	0.222	0.177	0.601
7 wt.% <i>f</i> -MWCNTs-PVDF	0.075	0.131	0.794
5 wt.% MNT-PVDF	0.530	0.1	0.370
7 wt.% MNT-PVDF	0.608	0.1	0.292
5 wt.% MNT-1 wt.% <i>f</i> -MWCNTs-PVDF	0.780	0.01	0.210
7 wt.% MNT-1 wt.% <i>f</i> -MWCNTs-PVDF	0.796	0.01	0.194

matrix. The incorporation of MNTs in *f*-MWCNT-PVDF composite helps in overcoming the Van der Waals forces between *f*-MWCNTs while utilizing the high aspect ratio of them. Another advantage of the addition of MNTs is that it could decrease the amount of *f*-MWCNT loading in PVDF matrix.

### Conclusion

Novel hybrid nanofiller consisting of multiwalled carbon nanotubes and MnO<sub>2</sub> nanotubesreinforced PVDF composite has been fabricated and proposed as an efficient material for EMI shielding applications. MNTs and *f*-MWCNTs acting as spacers in PVDF matrix helps in reducing the aggregation of the nanofillers and creates an excellent 3 D conducting network in the polymer. MNTs are acting as very good filler material when added to the entangled carbon nanotubes incorporated polymer. An EMI shielding effectiveness of approximately 20 dB has been achieved with 5 wt.% MNTs and 1 wt.% *f*-MWCNTs in polymer matrix in X-band region. The increase in EMI shielding effectiveness with the addition of nanofillers is attributed to the enhanced electrical conductivity of the composite due to the addition of *f*-MWCNTs and good homogeneity of the nanofillers in the polymer. The present hybrid polymer nanocomposites are proposed as low-cost and efficient EMI shielding materials in X-band region.

### Acknowledgements

This work was supported by IIT Madras and the authors thank the Department of Science and Technology (DST), India for financial support. One of the authors (V. ESWARAIYAH) thanks Dr. Harishankar Ramachandran, professor, Microwave Lab, Department of Electrical Engineering, IIT Madras for helping in EMI shielding measurements.

### Author details

<sup>1</sup>Alternative Energy and Nanotechnology Laboratory (AENL), Nano Functional Materials, Technology Centre (NFMT), Department of Physics, Indian Institute of Technology Madras, Chennai 600036, India <sup>2</sup>Low Temperature Physics Laboratory, Department of Physics, Indian Institute of Technology Madras, Chennai 600036, India

### Authors' contributions

VER carried out the composites preparation, other characterizations and written the manuscript. VSN and SRP are conceived in its coordination. All authors read and approved the final manuscript.

### Competing interests

The authors declare that they have no competing interests.

Received: 10 October 2010 Accepted: 14 February 2011

Published: 14 February 2011

### References

1. Imai M, Akiyama K, Tanaka T, Sano E: Highly strong and conductive carbon nanotube/cellulose composite paper. *Compos Sci Technol* 2010, **70**:1564.
2. Chung DDL: Electromagnetic interference shielding effectiveness of carbon materials. *Carbon* 2001, **39**:279.
3. Azim SS, Satheesh A, Ramu KK, Ramu S, Venkatachari G: Studies on graphite based conductive paint coatings. *Prog Org Coat* 2006, **55**:1.

4. Database for chemical resistance of PVDF. [http://www.zeusinc.com/technicalservices/technicalbulletins/chemicalresistanceofpolymers/chemicalresistancechartpdf.aspx].
5. Steller J, Krella A, Koronowicz J, Janicki W: Towards quantitative assessment of material resistance to cavitation erosion. *Wear* 2005, **258**:604.
6. Wu M, Shaw LL: On the improved properties of injection-molded, carbon nanotube-filled PET/PVDF blends. *J Power Sources* 2004, **136**:37.
7. Lee Y-B, Lee C-H, Lim D-S: The electrical and corrosion properties of carbon nanotube coated 304 stainless steel/polymer composite as PEM fuel cell bipolar plates. *Int J Hydrogen Energy* 2009, **34**:9781.
8. Iijima S: Helical microtubules of graphitic carbon. *Nature* 1991, **354**:56.
9. Tersoff J, Ruoff RS: Structural Properties of a Carbon-Nanotube Crystal. *Phys Rev Lett* 1994, **73**:676.
10. O'Connell MJ: *Carbon nanotubes: Properties and Applications* Routledge: Taylor and Francis; 2006.
11. Barick AK, Tripathy DK: Effect of nanofiber on material properties of vapor-grown carbon nanofiber reinforced thermoplastic polyurethane (TPU/CNF) nanocomposites prepared by melt compounding. *Compos Part A* 2010, **41**:1471.
12. Salvatierra RV, Oliveira MM, Zarbin AJG: One-Pot Synthesis and Processing of Transparent, Conducting, and Freestanding Carbon Nanotubes/ Polyaniline Composite Films. *Chem Mater* 2010, **22**:5222.
13. Singh I, Madhwal D, Verma A, Kumar A, Rait S, Kaur I, Bharadwaj LM, Bhatia CS, Bhatnagar PK, Mathur PC: Enhanced luminance of MEH-PPV based PLEDs using single walled carbon nanotube composite as an electron transporting layer. *J Lumin* 2010, **130**:2157.
14. Cheng KB, Ramakrishna S, Lee KC: Electromagnetic shielding effectiveness of copper/glass fiber knitted fabric reinforced polypropylene composites. *Compos Part A* 2000, **31**:1039.
15. Kaynak A: Electromagnetic shielding effectiveness of galvanostatically synthesized conducting polypyrrole films in the 300-2000 MHz frequency range. *Mater Res Bull* 1996, **31**:845.
16. Coleman JN, Khan U, Blau WJ, Gun'ko YK: Small but strong: A review of the mechanical properties of carbon nanotube-polymer composites. *Carbon* 2006, **44**:1624.
17. Chen C, Lu Y, Kong ES, Zhang Y, Lee ST: Nanowelded Carbon-Nanotube-Based Solar Microcells. *Small* 2008, **4**:1313.
18. Al-Saleh MH, Sundararaj U: Electromagnetic interference shielding mechanisms of CNT/polymer composites. *Carbon* 2009, **47**:1738.
19. Han MS, Lee YK, Lee HS, Yun CH, Kim WN: Electrical, morphological and rheological properties of carbon nanotube composites with polyethylene and poly(phenylene sulfide) by melt mixing. *Chem Eng Sci* 2009, **64**:4649.
20. Panwar V, Kang B, Park JO, Park S, Mehra RM: Study of dielectric properties of styrene-acrylonitrile graphite sheets composites in low and high frequency region. *Eur Polym J* 2009, **45**:1777.
21. Panwar V, Park JO, Park SH, Kumar S, Mehra RM: Electrical, dielectric, and electromagnetic shielding properties of polypropylene-graphite composites. *J Appl Polym Sci* 2010, **115**:1306.
22. Chen LM, Ozisik R, Schadler LS: The influence of carbon nanotube aspect ratio on the foam morphology of MWNT/PMMA nanocomposite foams. *Polymer* 2010, **51**:2368.
23. Jou W-S, Cheng H-Z, Hsu C-F: The electromagnetic shielding effectiveness of carbon nanotubes polymer composites. *J Alloys Compd* 2007, **434**:641.
24. Yun J, Im JS, Lee Y-S, Kim H-I: Effect of oxyfluorination on electromagnetic interference shielding behavior of MWCNT/PVA/PAAC composite microcapsules. *Eur Polym J* 2010, **46**:900.
25. Xiang C, Pan Y, Guo J: Electromagnetic interference shielding effectiveness of multiwalled carbon nanotube reinforced fused silica composites. *Ceram Int* 2007, **33**:1293.
26. Li Y, Chen C, Zhang S, Ni Y, Huang J: Electrical conductivity and electromagnetic interference shielding characteristics of multiwalled carbon nanotube filled polyacrylate composite films. *Appl Surf Sci* 2008, **254**:5766.
27. Mathur RB, Pande S, Singh BP, Dhami TL: Electrical and mechanical properties of multi-walled carbon nanotubes reinforced PMMA and PS composites. *Polym Compos* 2008, **29**:717.
28. Pande S, Singh BP, Mathur RB, Dhami TL, Saini P, Dhawan SK: Improved Electromagnetic Interference Shielding Properties of MWCNT-PMMA Composites Using Layered Structures. *Nanoscale Res Lett* 2009, **4**:327.
29. Li Y, Chen CX, Li JT, Zhang S, Ni YW, Cai S, Huang J: Enhanced Dielectric Constant for Efficient Electromagnetic Shielding Based on Carbon-Nanotube-Added Styrene Acrylic Emulsion Based Composite. *Nanoscale Res Lett* 2010, **5**:1170.
30. Yang YL, Gupta MC, Dudley KL, Lawrence RW: A comparative study of EMI shielding properties of carbon nanofiber and multi-walled carbon nanotube filled polymer composites. *J Nanosci Nanotechnol* 2005, **5**:927.
31. Yang Y, Gupta MC, Dudley KL: Towards cost-efficient EMI shielding materials using carbon nanostructure-based nanocomposites. *Nanotechnology* 2007, **18**:345701.
32. Reddy ALM, Shajjumon MM, Ramaprabhu S: Alloy hydride catalyst route for the synthesis of single-walled carbon nanotubes, multi-walled carbon nanotubes and magnetic metal-filled multi-walled carbon nanotubes. *Nanotechnology* 2006, **17**:5299.
33. Xiao W, Xia H, Fuh JYH, Lu L: Growth of single-crystal [alpha]-MnO2 nanotubes prepared by a hydrothermal route and their electrochemical properties. *J Power Sources* 2009, **193**:935.
34. Li N, Huang Y, Du F, He XB, Lin X, Gao HJ, Ma YF, Li FF, Chen YS, Eklund PC: Electromagnetic Interference (EMI) Shielding of Single-Walled Carbon Nanotube Epoxy Composites. *Nano Lett* 2006, **6**:1141.

doi:10.1186/1556-276X-6-137

Cite this article as: Eswaraiyah et al: Inorganic nanotubes reinforced polyvinylidene fluoride composites as low-cost electromagnetic interference shielding materials. *Nanoscale Research Letters* 2011 **6**:137.

Submit your manuscript to a SpringerOpen® journal and benefit from:

- Convenient online submission
- Rigorous peer review
- Immediate publication on acceptance
- Open access: articles freely available online
- High visibility within the field
- Retaining the copyright to your article

Submit your next manuscript at ► [springeropen.com](http://springeropen.com)